

# COMPUTER MODELING OF CASTINGS QUALITY WITH TAKING INTO ACCOUNT THE DIFFERENTIATION OF STRUCTURE-DEPENDENT CORES AND MOLDS MATERIAL PROPERTIES

МОДЕЛИРОВАНИЕ ПРОЦЕССОВ ФОРМИРОВАНИЯ КАЧЕСТВА ОТЛИВОК С УЧЁТОМ ДИФФЕРЕНЦИАЦИИ СТРУКТУРНО-ЗАВИСИМЫХ СВОЙСТВ ФОРМ И СТЕРЖНЕЙ

Dr. Broymant O.A.<sup>1</sup>, eng. Babkov D.S.<sup>2</sup>, Dr. Ioffe M.A.<sup>3</sup>

All-Union Centre for Transportation Technologies LLC<sup>1,2</sup>, Saint Petersburg Polytechnic University<sup>3</sup> – Russia

**Abstract:** Typical casting simulation procedure doesn't consider exact cores and molds material properties as a primary factor. Sometimes mold is considered as an isotropic body characterized with constant averaged thermophysical and other properties. On the other hand there are a lot of practically collected data confirming the fact that input of exact non-uniformly distributed thermophysical mold properties during casting simulation may seriously improve the prognosis of casting quality. The present work is dedicated to interconnections between molds compacting conditions and castings quality. It has been proposed to carry out the computer modeling of compacting process for further use of the calculation results as a part of input for casting simulation software.

**KEYWORDS:** COMPACTING, NON-UNIFORM STRUCTURE, FOUNDRY MOLDS AND CORES, SAND DENSITY, SAND PROPERTIES, CASTING SIMULATION.

## 1. Introduction

Common use of casting simulation software (CSS) involves necessity of a knowledge database for material properties and initial data considered as the part of mathematical models that form a basis of CSS. Accuracy of the data defines adequacy for casting quality prediction. The data consists of molds and cores properties, which are non-uniformly distributed in compacted sand due to its structure differentiation, temperature anisotropy and local material transformations. Taking into account the spatial distribution of thermophysical, filtration and other mold properties provides significant increase of CSS use effectiveness.

## 2. Computer modeling of sands compacting process

Degree of sand compaction is one of the main characteristics for mold quality, which directly affects to casting quality. Evident demands to foundry mold are connected to necessity in satisfactory dimensional accuracy and sand mechanical properties. Besides of that, non-uniform structure of compacted sand establishes complex conditions for gas and moisture migration, heat transfer from casting, etc.

Empirical and analytical solutions for sand compacting were obtained during, basically, 60's-70's of previous century [1-4]. In modern times the sand compacting problem for arbitrary shape tooling may be successfully solved with a numerical simulation analysis in the special Arena-flow software [5], or appropriate modulus in CSS ProCast, MagmaSoft [6, 7] or in multipurpose finite-element software [8-10]. In the present work numerical analysis of sand compacting during its pressing was performed in NX Advanced Simulation application. Sand was considered as a linearly elastic body, which is, as shown in number of works, allowable assumption in case of a single load and if stress values lay in a certain range [3].

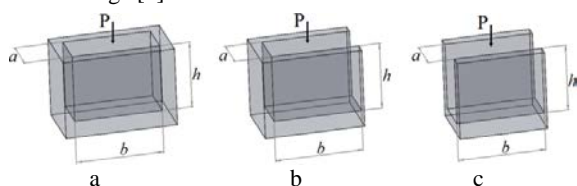


**Figure 1:** Types of pockets configuration:  
a – one-sided; b – two-sided; c – three-sided

Considering replication of a pattern profile, the particular interest is in reaching a sufficient sand density in so called pockets which may exist in pattern itself, gaps between pattern and flask wall, etc. Three types of pockets [4] could be defined (Fig. 1). The most complex pocket is one-sided if ram from the top. Appropriate

molding pressure for reaching the sufficient sand density on the pocket bottom depends on proportions between main sizes  $a$ ,  $b$  and  $h$ .

Mix compositions and properties of sands [3] compacting of which has been investigated in the present work are summarized in the Table 1:  $E$  – structural strain modulus (analogue of Young's modulus);  $\mu$  – transverse strain ratio (analogue of Poisson number);  $\rho_0$  – initial density of the mix. Coefficient of contact friction between sand and pattern walls was assumed  $f=0,20-0,35$ . Mechanical properties of sands were determined experimentally for triaxial compression material state. As for initial density, which is, in the general case, non-uniformly distributed within the sand prior to its pressing, the task may be solved with molds and cores blowing simulation software.

Nr.	Addition, % wt.			$\rho_0$ , kg/m <sup>3</sup>	$E$ , MPa	$\mu$
	Sand K016 (95 AFS)	Clay	Water			
1	-	-	-	1500	170	0,32
2	100	-	3,5	1240	37	
3		10,0	2,5	1200	9,3	
4		12,0	3,0	1450	17,5	

**Table 1:** Mix composition and properties of investigated sands

Strains in the system obtained through finite-element analysis of sand strain-stressed state during pressing procedure allowed identifying the ratio between initial  $V_0$  and final  $V$  local volumes in the depth of sand pack. Local (inside the element) effective density  $\rho$  distribution was calculated through the criteria analysis option embedded into the software postprocessor by the next evident formula:

$$\rho = \rho_0 \frac{V_0}{V} \quad (1)$$

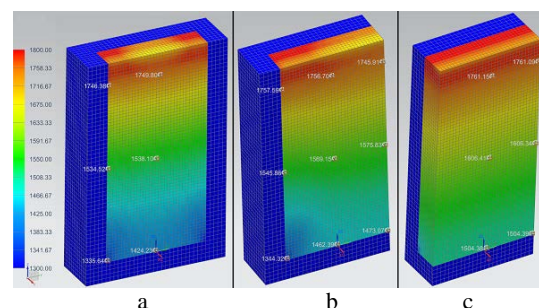


**Figure 2:** Sand Nr. 3 density distribution (kg/m<sup>3</sup>) after pressing in differently configured pockets (cross-sectional view,  $\rho$  values are marked for selected regions):  
a – one-sided; b – two-sided; c – three-sided

Fig. 2 shows sand Nr. 3 density distribution in the moderately deep pockets ( $a:b:h=1:2:4$ ) of different shape for compacting pressure  $P=1$  MPa. Sand density increases, in particular at the bottom, along with simplification of the pocket type. Satisfactory sand density (depending on demands, equals to 70-90% from maximum possible  $\rho_{sc}$ ) at the bottom, i.e. in the working area which directly contacts to liquid metal, could be observed for the selected pressure and system sizes in the case of three-sided pockets; other cases show necessity for compacting pressure increase.

Density distribution calculation results for one-sided pocket ( $a:b:h=1:2:4$ ) are shown in Fig. 3. Clay-bonded sands compactability depends on, first of all, initial density, clay and water content. Dry silica sand shows low compactability which could be improved with water addition.

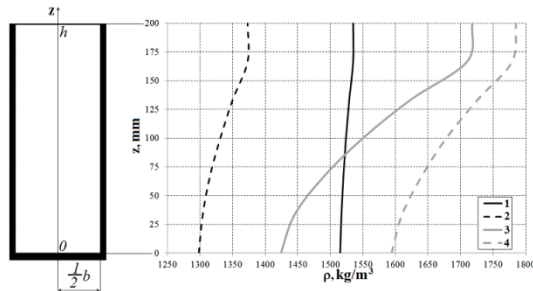


**Figure 3:** Density distribution on the axial line of one-sided pocket for sands Nr. 1-4 pressing cases

Non-uniform density distribution is a reason for spatial non-uniformity of other sand properties. Fig. 4, a shows calculated prediction of a spatial distribution of locally-effective (within every element) heat conductivity coefficient  $\lambda$  and volumetric heat capacity  $C_v$  of compacted sand. The prediction is based on special structure models of bonded sands [11] developed on the granular media averaged cell approach [12]. Express-estimation for gas permeability  $K_g$  was performed with a further mentioned criteria analysis comfortable option which allows instant plotting the full

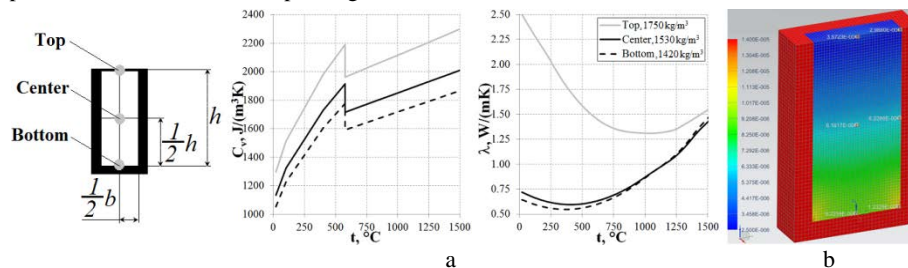


**Figure 4:** Calculative prediction for structure-dependent properties of sand Nr. 3 after its compacting in one-sided pocket:  
a – temperature-dependent thermophysical properties in the axial line regions;  
b – gas permeability distribution ( $m^2/(N \cdot s)$ ) at normal temperature (cross-sectional view)

Non-uniform distribution of sand thermophysical properties and gas permeability, furthermore which are instable during mold heating due to structural transformations (volumetric changes of mix components, thermal decomposition, evaporation and condensation of moisture, etc.), leads to nontrivial thermal and gaseous regimes of the mold, so all of that circumstances influence on cast result in a complicated way.

### 3. Numerical simulation of castings with taking into account the non-uniform mold structure

The above-mentioned mold and core production simulation software prognoses completeness of occupancy of tooling cavities and differentiating in density distribution. As a result of work with the software tools Based on the analysis made with the aids of special software an optimal tooling design and blowing regime could be developed. At the same time the calculated data on non-uniform mold structure cannot be further utilized during casting simulation procedure. At this stage the data is lost and mold is considered as a quasiisotropic body, at the best case endowed with temperature-dependent, but not spatial-dependent, thermophysical properties. However, it seems reasonable to inherit previously

field of calculated value on the three-dimensional model (Fig. 4, b). The user formula [13] utilized for the criteria analysis is similar to known Kozeny–Carman equation:

$$K_g = \frac{d^2 m^3}{36 \xi \mu_g (1-m)^2 (3-m)}, \quad (2)$$

where  $m$  – sand porosity calculated from the evident proportions between  $\rho$  and individual densities of mix components;  $d$  – sand particles size;  $\xi$  – pore tortuosity (for typical foundry sand mixes it could be assumed, in average [13],  $\xi=1.5$ );  $\mu_g$  – dynamic-viscosity coefficient. Spatial distribution for  $K_g$  is essential for mold gaseous regime calculations through appropriate differential equations [9, 13].

Effective conductivity value (Fig. 4, a) for overcompacted sand in the top pocket zone ( $m \sim 0.36$ ) is influenced significantly by individual conductivities of solid components of sand, at the same time radiative transfer is depressed due to relatively low pore amount. Other situation is observed in the moderately compacted layer at the pocket bottom ( $m \sim 0.47$ ): in the range of low and medium temperatures  $t$  sand conductivity is relatively low due to weak contact interactions between mix particles, while in the range of high temperatures conductivity rises actively due to intensification of radiative transfer in sand pores. Effective volumetric heat capacity rises evidently with a growth of sand density.

Sand gas permeability (Fig. 4, b) decreases with increasing of the distance from the pocket bottom, which is not complied with recommendation based on the abstract concept for favorable gas transport conditions. The evident recommendation says that  $K_g$  must increase with increasing of the distance from the mold working surface which will be in contact with liquid metal. In general case it is recommended [1] to have uniform distribution of  $K_g$  in the mold volume (i.e. uniform distribution of  $\rho$ ); well-grounded selection of optimal compacting conditions may help to get near that.

obtained calculative results for molds and cores structure, arrange appropriate differentiate assigning of thermophysical and filtration mold properties distribution for further casting simulation with improved accuracy.

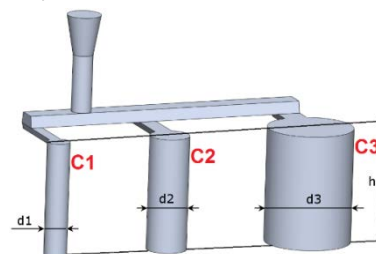


**Figure 5:** Cylinder sample castings

In order to determine how much the density non-uniformity may affect on cast result a number of computational experiments with a cylinder sample castings (Fig. 5, identification marks for cylinders are C1, C2, C3 as long as their diameter is increased) were carried out. The cylinders are produced of different alloys (Table 2) in clay-bonded molds compacted with different pressure. The mold for cylinders includes a sort of three-sided

pockets so the degree of compacting in them will vary after pressure differences.

Nr.	Alloy type	Alloy grade (Rus)	Solidification range, °C
1	Hypereutectic silumin	AK18	670-560
2	Grey iron	SCh30	1220-1150
3	Carbon steel	20L	1530-1480

Table 2: Foundry alloys for cylinder sample castings production

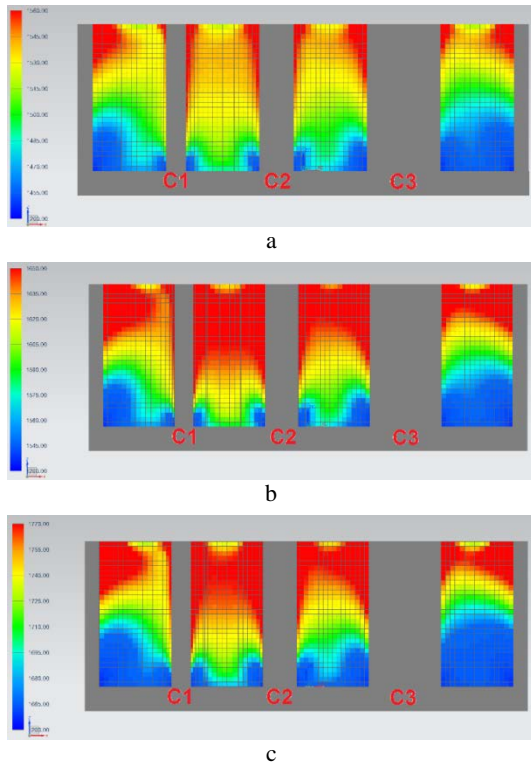


Figure 6: Sand density differentiation (cross-sectional view) in three-sided pockets around cylindrical elements of the pattern (h=200 mm, Ø40 mm – C1, Ø70 mm – C2, Ø150 mm – C3) as a result of sand Nr. 3 compacting calculations with different pressures: 0,6 MPa (a), 0,8 MPa (b) u 1,0 MPa (c)

Compacting of sand Nr. 3 was considered as a method for cylinder sample casting mold production. Three-dimensional analysis in NX Advanced Simulation was utilized to predict sand non-uniform structure within the mold (Fig. 6), the data was further taken into account during castings simulations in CSS PolygonSoft. To arrange the inheritance procedure calculated density fields after converting in specially made program and additional adaptational mesh converting in Altair HyperMesh software were transformed to finite-element geometry data (Fig. 7). For every mold layer fixed density was assigned which is acceptable assumption due to modest variation of density within the each layer (10-20 kg/m<sup>3</sup>). Individual temperature-dependent thermophysical properties ( $\lambda$  and  $C_p$ ) of each layer were calculated on the basis of of the structure models [11]

taking into account appropriate densities. These properties were further utilized during solidification analysis of cylinder sample castings of different diameter. In order to prevent influence on calculation results from heat loss on cylinders end boundaries (top and bottom) these planar surfaces were assigned as adiabatic.

As a result of the castings simulations full solidification times and solidification sequences were discovered for each sample cylinder solidified in non-uniformly structured mold. The obtained data was compared with typical results of CSS analysis when the mold is assigned with stable uniform density and appropriate temperature-dependent thermophysical properties. However, the uniform density for each case was defined in reasonable way – the effective value was calculated as an average weighted among all densities previously calculated for each mesh element. That made the result equal to known method for density measuring through sand mold weighting procedure.

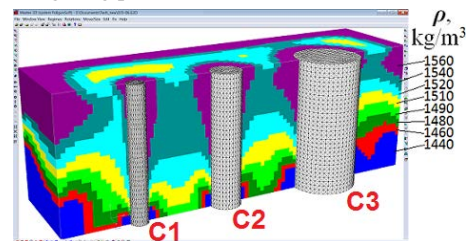


Figure 7: Calculated mold density fields obtained from compacting modeling in transformed view which represents finite-element geometry for casting in the complex structured mold plotted in CSS preprocessor (example for compacting at 0,6 MPa)

Calculation results for test cylinders solidification times are summarized in Table 3. Pressure rise leads to decrease of solidification times due to general increase of mold heat-removing ability. However, the situation isn't as trivial for thick cylinders solidification. In this case the mold experiences deeper heating so the volume of sand, which affects on general heat exchange in the casting-mold system, is significant. In accordance to the run of thermophysical properties curves, the properties could rise or descend with a temperature increase in each layer. Therefore, if overall sand density is slightly raised massive castings may solidify the same time or even a bit longer than in the case of mold with a slightly lower density. Considering complex castings, it must be taken into account that neighboring elements of the casting may affect each other through appropriate mold regions; the regions are able to heat-up faster and deeper in consequence of overall increase of thermophysical properties.

Solidification times vary significantly from one alloy to another which is not only connected to solidification range, individual alloy thermophysical properties, interval between pouring and initial mold temperatures which results in faster cooling of high-temperature alloys, etc. Additional reason for the variety is significant difference in sand thermophysical properties when mold is heating from different initial temperatures of an alloy. In such a way radiative transfer isn't affect as much in case of aluminum alloy pouring in comparison with steel pouring – however, the effect isn't so evident in case of highly compacted sand.

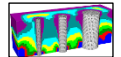
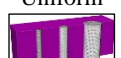
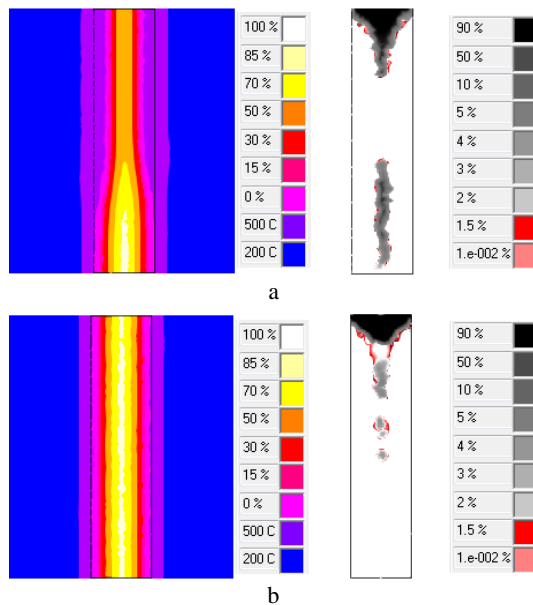
Mold properties distribution	Alloy	Cylinders solidification times, s								
		C1, Ø40 mm			C2, Ø70 mm			C3, Ø150 mm		
		0,6 MPa	0,8 MPa	1,0 MPa	0,6 MPa	0,8 MPa	1,0 MPa	0,6 MPa	0,8 MPa	1,0 MPa
 Non-uniform	AK18	553	445	200	1622	1020	552	7380	4879	2416
	SCh30	322	303	176	922	849	495	4048	3680	2169
	20L	190	181	125	531	505	346	2269	2154	1495
 Uniform	AK18	541	488	183	1603	1443	513	7257	6512	2237
	SCh30	311	293	157	895	839	444	3931	3683	1933
	20L	185	177	114	518	494	314	2222	2118	1348

Table 3: Solidification times for test castings produced in differently compacted molds

Solidification analysis for castings in molds with well-defined material properties anisotropy is considered as more accurate in comparison with traditional casting simulation practice when the

mold appears as "equivalent" isotropic body. Comparison result for the cases shows good agreement between calculated solidification times – average difference is about 10%. The main reason for that is

well-grounded averaging for isotropic mold effective density. Increase of solidification time, as well as test cylinder diameter, and its height (as shown with additional calculations in this case difference between top and bottom densities may increase dramatically) lead to much more significant solidification time mismatching.



**Figure 8:** Solidification of steel test cylinder of  $\varnothing 70$  mm in differently structured molds pressed at 0,8 MPa:  
*a* – typical liquid phase distribution at intermediate moment of casting cooling in anisotropic mold and final porosity prognosis;  
*b* – the same for “equivalent” isotropic mold

Undoubtedly, consideration of solidification time differences is insufficient to ground or deny applicability of traditional isotropic mold approach. In addition to that, solidification sequence must be considered. The sequence is critical for solidification directionality, tendency to defects formation, features of metal structure, for example, local chilling on iron castings, etc. Fig. 8, a shows liquid phase distribution at intermediate moment of cylinder solidification in the mold with non-uniformly distributed density decreased from top to bottom and appropriate porosity prognosis. The result is clearly not a same as the idealized case of solidification in the mold with uniform density distribution (Fig. 8, b). In the first case hot spot migrates to bottom region which leads to porosity located under  $1/2h$  level while idealized case shows porosity above the level only.

#### 4. Conclusion

The present investigation proves reasonability of casting simulation procedure improving through taking into account the data on foundry molds non-uniformly compacted structure. This allows increasing calculation accuracy for heat-transfer and metal flow processes, gaseous regime in casting-mold system, etc. The approach offers opportunity to solve a number of problems connected to mold-dependent casting defects on new improved level of quality. Development of the approach is connected to, first of all, creation of sustainable interface for data exchange between computer modeling software, improving the mathematical models for sand compacting as well as for sand structure and material properties transforming after the melt is poured into the mold.

#### References

- [1] Орлов Г.М. Автоматизация и механизация процесса изготовления литейных форм. – М.: Машиностроение, 1988. – 264 с.
- [2] Ангелов Г., Иванов П., Македонски З., Добрев П. Съвременни методи за изработване на леярски сърца. – София: Техника, 1975. – 295 с.
- [3] Корнюшкин О.А., Иоффе М.А. Исследование характеристик механических свойств формовочных смесей. //Изв. вузов. Машиностроение, 1976 – 6, с. 126-130
- [4] Tilch, W.: Ermittlung Verfahrensbedingter Sortimentsgrenzen und Optimierung der Formstoffzusammensetzung für das Hochdruckpressen; Freiberg Forschungsh, 1973, B, No. 179
- [5] Snider, D.M.: Three Fundamental Granular Flow Experiments and CPFD Predictions; Powder Technology, 2007, No. 176, p. 36–46
- [6] J. Dańko, J.; Dańko, R.; Burbelko, A.; Skrzyński, M.: Parameters of the Two-Phase Sand-Air Stream in the Blowing Process; Archives of Foundry Engineering, 2012, vol. 12, No. 4, p. 25-30
- [7] Sturm, J.C.; Wagner, I.: Praktischer Einsatz der Kernsimulation zur Prozessoptimierung; Giesserei-Rundschau, 2012, No. 59, p. 246-252
- [8] Бройтман О.А., Иоффе М.А., Шевченко Д.В. Формирование структурно-зависимых свойств формовочной смеси при уплотнении. //Литейщик России, 2014 – 1, с. 20-23
- [9] Бройтман О.А., Крупников А.В., Иоффе М.А., Шевченко Д.В. Газопроницаемость неравномерно уплотнённого материала литейной формы. //Труды X международной научно-практической конференции «Литейное производство сегодня и завтра». СПб.: Изд-во СПбГПУ, 2014, с. 277-285
- [10] Lia, W.; Wu, J.: Numerical Simulation of Compacting Process of Green Sand Molding Based on Sand Filling; Materials Science Forum, 2007, vols. 561-565, p. 1879-1882
- [11] Бройтман О.А. Моделирование структуры и распространения тепла в дисперсных формовочных материалах для прогноза их теплофизических свойств. //Сб. Компьютерный анализ литейной технологии: проблемы и перспективы. СПб.: ЦНТИ Прогресс, 2007, с. 15-25
- [12] Dulnev, G.N.; Zarichnyak, Yu. P.; Muratova, B. L.: The Thermal Conductivity of Granular and Weakly Sintered Materials. Journal of Engineering Physics, 1969, vol. 16, No. 6, p. 697-704
- [13] Серебро В.С. Основы теории газовых процессов в литейной форме. – М.: Машиностроение, 1991. – 208 с.